NASA TECHNICAL MEMORANDUM

NASA TM X-68228

NASA TM X-68228

A POTENTIAL MEANS OF USING ACOUSTIC EMISSION FOR CRACK DETECTION UNDER CYCLIC-LOAD CONDITIONS

by Alex Vary and Stanley J. Klima
Lewis Research Center
Cleveland, Ohio

TECHNICAL PAPER proposed for presentation at
Ninth Symposium on Nondestructive Evaluation
San Antonio, Texas, April 25-27, 1973

A POTENTIAL MEANS OF USING ACOUSTIC EMISSION FOR CRACK DETECTION UNDER CYCLIC-LOAD CONDITIONS

Alex Vary and Stanley J. Klima
Lewis Research Center
National Aeronautics and Space Administration
Cleveland, Ohio

E-7431

Abstract

A preliminary investigation was conducted to assess the feasibility of monitoring acoustic emission signals from fatigue cracks during cyclic bend tests. Plate specimens of 6Al-4V titanium, 2219-T87 aluminum, and 18-Ni maraging steel were tested with and without crack starter notches. It was found that significant acoustic emission signals could be detected in the frequency range from 100 kHz to 400 kHz. Cracks emanating from starter notches were monitored by the ultrasonic pulse-echo technique and periodically measured by micro-optical examination. Methods used to reduce the effects of extraneous noises (i.e., machine noises, fretting) are described. A frequency spectrum analyzer was used to characterize the emissions and to evaluate methods used to acquire the signals (i.e., transducer location, bandwidth selection). The investigation indicated that it was possible to extract meaningful acoustic emission signals in a cyclic bend machine environment.

1. INTRODUCTION

This paper describes a study of acoustic emission signals emitted during fatigue cracking of plate specimens subjected to cyclic bending at 19 Hz. The study was conducted with plate specimens of 6Al-4V titanium, 2219-T87 aluminum, and 18-Ni maraging steel. A specific goal of this study was to determine the conditions required in a cyclic bend machine for acquiring meaningful acoustic emission signals from fatigue specimens. A further goal was to use this device to conduct a preliminary investigation of the characteristics of the acoustic emissions produced by selected representative materials.

A high-speed bending fatigue machine was selected for this study because it permits the use of a simple specimen configuration and simulates the loading conditions found in many actual components. However, a high-speed fatigue machine is an inherently noisy device in which extraneous signals can become superimposed on and thus mask signals generated by the test specimen. One purpose of this report is to show that meaningful acoustic emissions can be extracted from this noisy environment and that continuous monitoring of acoustic emissions in this type of environment is a potentially useful tool for investigating fatigue cracking.

Acoustic emission has been frequently cited as a means for fatigue crack detection and investigation.[1-4] Previous studies by others have indicated that significant acoustic emission signals can be extracted from noisy environments, as for example in arc welding, die forming, and nuclear machinery involving hydraulic background noises.[5-6] This is possible because significant signals often arise within frequency bands that are different from the extraneous and background vibrations. Other investigators have circumvented the background noise problem by devising "spatial filtering" networks that discriminate against extraneous signals by keeping track of signal arrival times or coincidences.[7-8] Cyclic noises also have been avoided by periodically interrupting fatigue tests and measuring acoustic emissions during monotonic "proof" loading of the fatigue specimen.[9-10]

However, acoustic emission studies of subcritical crack growth have predominantly been confined to situations in which growth was induced by monotonic loading alone. Only recently have investigators undertaken continuous crack growth monitoring via acoustic emissions under cyclic loading conditions.[11-13] However, these previous tests have been conducted in tensile

machines under axial loading which involve elaborate precautions to prevent machine and grip noises from interfering with the crack noises. The cyclic bender on the other hand appears to offer considerably greater simplicity for conducting cyclic fatigue crack growth studies. Use of a plate bender for this purpose should provide the kind of information that is needed to correctly assess the applicability of acoustic emission methods for crack detection and crack growth monitoring in cyclically-loaded structures.[14]

2. TEST APPARATUS AND SPECIMENS

2.1 TEST APPARATUS

The equipment used in these tests consisted of two main devices: (1) a cam-operated bending fatigue machine, and (2) an acoustic emission system. Associated equipment included an ultrasonic probe unit and a frequency-spectrum analyzer. The fatigue machine, a plate test specimen, and acoustic emission and ultrasonic transducers are shown in Fig. 1.

One end of the specimen was held in a stationary vise that was rigidly mounted on a table as illustrated in Fig. 2. The opposite end of the specimen was held in a foreclamp that extended under two cams that are identified in Fig. 1 and illustrated in Fig. 2(b). These cams were eccentric with respect to the motor-driven shaft and bore upon the foreclamp exerting a downward force with each cycle of the motor. The cams flexed the specimen at a rate of 19 Hz. The cam throw or specimen displacement was not variable; therefore, the strain range at any point along the specimen was the same for all specimens tested. The cams had free rolling rims in contact with the foreclamp so that there was no relative motion between the cam rims and foreclamp. The maximum flexural load was controlled by stacking shims under the specimen in the vise as indicated in Fig. 2(b). Rubber and teflon sheets were inserted between the specimen and clamp plates to serve as acoustic buffers to minimize extraneous noise and to eliminate fretting between the specimen and vise.

The top plate of the vise contained holes for installing acoustic emission and ultrasonic transducers at appropriate locations on the specimen as indicated in Fig. 2(a). The ultrasonic transducer was mounted on an angle block (plastic wedge) to produce shear waves in the specimen and positioned so that it could receive echos from a specific region on the specimen. This region was the crack starter notch indicated in Fig. 2(a). Ultrasonic pulses were sent to and reflected from the notch region along the path indicated by the dotted line in Fig. 2(b). The ultrasonic transducer operated at a frequency of 5 MHz and was used to monitor crack initiation and growth of fracture surfaces originating from the starter notch.

The schematic in Fig. 3 shows a block diagram of the acoustic emission system. Two transducers were used to monitor acoustic emissions that originated in the specimen as well as other sources. Each acoustic emission channel (A and B) contained a differential preamplifier that raised the signal amplitude by a factor of 100 (40 dB). In addition to broadband capability, each channel had bandpass filters that afforded a selection of four frequency ranges: 100 kHz to 2 MHz, 100 to 300 kHz, 300 kHz to 1 MHz, and 1 to 2 MHz. Each channel contained a variable postamplifier that provided for additional signal gain up to 60 dB in one decibel increments. The digital counters summed all received signals having amplitudes greater than 1 V and provided a DC output (via digital to analog converters) that was proportional to the contents of the counter sections. These two channels thus provided the cumulative acoustic emission counts plotted on the Y and Y' axes while a ramp generator provided a time base signal on the X axis of an X, Y, Y' plotter. A local oscillator, mixer, audio amplifier and speaker were used to heterodyne signals in the range from 100 to 300 KHz into the audio range. Acoustic emissions in this range therefore could be heard by ear as the tests progressed.

2.2 TEST SPECIMENS

The materials tested in this study were standard commercial grades of: 6Al-4V titanium (mill annealed), 2219-T87 aluminum, and 18Ni maraging steel. The maraging steel was heat treated to provide a yield strength of approximately 1300 N/m^2 (190 ksi). These materials were tested in the form of plate specimens approximately 7.6 cm (3 in.) wide by 30.5 cm (12 in.) long and 1.3 cm (0.5 in.) thick. The surface finish of these plates varied with the material. For example: the titanium alloy surface was in the as-rolled condition with fine homogeneous pitting; the aluminum alloy surface had a smooth, cold-worked, mill finish; and the maraging steel surface had a ground 32 rms finish.

Crack starter notches were electric discharge machined into the specimens as indicated in Fig. 2(a). The notches were between 0.1 cm (0.04 in.) and 0.2 cm (0.08 in.) long, 0.05 cm (0.02 in.) to 0.1 cm (0.04 in.) deep, and approximately 0.018 cm (0.007 in.) wide. The notches were "V"-shaped in a plane perpendicular to the specimen longitudinal axis.

3. EXPERIMENTAL PROCEDURE

3.1 BACKGROUND NOISE MEASUREMENTS

Preliminary testing was conducted to assess sources of noise in the plate bending machine. It was necessary to control the transmission of noise and extraneous acoustic signals from various sources. This was done by inserting buffering materials between the specimen and the vise and foreclamp plates (see fig. 2).

In the vise, the buffering was accomplished with 0.16 cm (0.063 in.) thick teflon sheets. In

particular, this helped eliminate fretting of the specimen at the edge of the vice clamp and thus the attendant extraneous noises. Rubber sheets 0.16 cm (0.063 in.) thick were used between the specimen and foreclamp plates.

In some trail cases the specimen was warped or nonuniformly clamped. This resulted in canting of the foreclamp and intermittent or poor contact with the cam rim during cycling. The result was either pounding, slipping, or rachetting and thus intolerable extraneous noises. Preliminary testing indicated that the contacts had to be balanced so that each cam exerted approximately equal force on the foreclamp throughout a cycle.

After measures were taken to set up a specimen with the previously mentioned buffering and load balancing, tests were conducted to assess the viability of the acoustic emission transducer placement indicated in Fig. 2. The procedure involved a fixed location for transducer A, as shown in Fig. 4. Transducer B was stationed at various test locations as indicated in the same figure. For this procedure, an unnotched plate specimen was used. With both sensors at their normal locations, tests were conducted to determine instrument settings for which both sensors responded equivalently for each of the four frequency bands. Next, sensor B was placed at test location No. 1. This provided relative response information with the sensor approximately 2.5 cm (1 in.) from the starter-notch site. Test location No. 2 provided data on noise primarily due to the cams, while test location No. 3 provided data primarily on bearing noises.

3.2 CRACK GROWTH MEASUREMENT PROCEDURES

The principle method of crack growth measurement was by means of a X7.5 to X30 variable magnification microscope fixture. A second method involved the previously described ultrasonic probe.

The optical method gave direct length measurements of cracks that emanated from either side of the starter notch. It also provided evidence of crack formation at the bottom of the notch. However, the latter was treated only as a qualitative data, and only actual surface crack lengths are reported herein.

The ultrasonic probe was used to monitor crack growth by reflections from the fracture surface (using the techniques described in ref. 15). The function served by this prove was to provide data on the continuity or lack of continuity (i.e., intermittance) of crack growth. Ultrasonic crack growth monitoring was applied simultaneously with acoustic emission monitoring for a few specimens. For other specimens ultrasonic crack monitoring was used alone. In either case, the ultrasonic probing was applied to a number of specimens in order to ascertain the mode of crack growth at early stages and to demonstrate that the ultrasound may be introduced while simultaneously monitoring acoustic emission signals without obscuring them.

By continuous ultrasonic monitoring of crack growth, it was observed that the cracks grew uniformly. That is, although there were abrupt increases in the acoustic emission count rate, the ultrasonic signals indicated only a smooth increase in crack size. This observation could be made for cracks with total surface lengths up to about 2 cm (~0.8 in.). Beyond this, limitations were imposed by the transducer crystal size and response characteristics.(15)

3.3 SPECIMEN TESTING PROCEDURE

Preliminary tests were conducted to assess the relative magnitude and frequency content of background noise. As a result, appropriate filter and gain settings for the acoustic emission sensors were determined. Channel A was set for the bandwidth from 100 kHz to 300 kHz and channel B from 300 kHz to 1 MHz.

The specimen test procedure consisted of two main parts: one set of specimens was for crack growth to full fracture; another set was for minimal crack growth (to about 0.1 cm (0.05 in.) total crack length).

The first part of the test procedure was devised to characterize the overall acoustic emission for specimens cycled to failure. This set was initially cycled without a starter notch in order to observe acoustic emissions from the intact specimen. Each of these specimens was then removed from the bender, electric discharge-notched, returned to the bender, and cycled until the specimen could be broken in two by hand. Correlation of the fracture surface texture with the acoustic emission data was one objective of this part of the test procedure. The other objective was to demonstrate the difference in acoustic emission signals from unnotched and notched specimens.

The second part of the test procedure was devised to determine the sensitivity of the acoustic emission system for detecting crack formation at the early stages. For the second set of specimens, both sensors were placed closer to the starter notch (that is, at test location No. 1 shown in fig. 4). Thus while the normal locations of sensors A and B were approximately 15 cm (6 in.) from the notch, in this part of the test they were about 2.5 cm (1 in.) from the notch. In addition, the specimen loading was substantially less than in the previously described part of the test procedure. The purpose of these measures was to induce slower crack formation and to characterize subtle variation in acoustic emission associated with crack formation. The specimens in this set were not taken to failure because they were destined for nondestructive evaluations by other techniques (not reported herein).

4. RESULTS

4.1 ACOUSTIC EMISSION DURING CRACK GROWTH

The acoustic emission and crack growth characteristics for three specimens are presented in Figs. 5, 6, and 7. The acoustic emission data are plotted as cumulative counts versus bend cycles. Coplotted in each figure are the optical measurements of the lengths of the cracks emanating from either side of the starter notch. This is identified on the abscissa as the "half-crack length." Generally, a crack appeared at the bottom of the notch first, but optical measurements were made only after it emerged on the specimen surface. The cracks usually extended approximately equally on each side of the notch and ran roughly parallel to the edge of the vise clamp. The total crack length could be taken as the sum of the two half-crack lengths plus the length of the starter notch. However, it was deemed sufficient herein to simply cite the actual surface measurements as an indication of crack growth versus bend cycles. This set of tests allowed the cracks to extend to the edges of the specimen (i.e., half-crack lengths of 3.8 cm (1.5 in.)) and then down the edges on each side until fracture occurred or was imminent. Results of this set of tests are summarized in table I, and corresponding photographs of the fracture surfaces appear in Fig. 8. Note also the acoustic emission count data for the unnotched condition of the titanium alloy and maraging steel specimens in Figs. 5 and 7.

Typical acoustic emission and crack growth characteristics are presented in Figs. 9 and 10 for "minimally-cracked" titanium and aluminum alloy specimens. As before, only crack dimensions that could be measured on the surface were taken even though evidence of initial cracking appeared inside the notch (at the bottom). These surface cracks were allowed to grow to no greater than about 0.06 cm (0.025 in.) "half-crack length" on either side of the notch.

4.2 FREQUENCY SPECTRA AND AUDIO EFFECTS

Frequency spectra in the two bands used for channels A and B were studied with a frequency-spectrum analyzer (fig. 3). A typical frequency spectrum is shown in Fig. 11 for a titanium alloy specimen. Similar spectra were obtained for the aluminum alloy specimens. Acoustic emission signals for the materials tested were most prominent in the 100 to 400 kHz band. Beyond this range, the signal amplitudes were at or below background levels.

During tests with notched specimens, when crack growth was in progress, the acoustic emissions were monitored by listening to the audio speaker (fig. 3). Specimens with cracks tended to produce distinct "sputtering" sounds against the normal background noise of the machine. This sputtering was fairly continuous in the case of titanium, for the full-fracture specimens. In aluminum full-fraction specimens, the sputtering occurred only near the last half of the test. But it was absent for the full-fracture maraging steel specimens. It was noted that when the sputtering occurred, the tallest peaks in the frequency-spectrum display (e.g., the 170 kHz peak in fig. 11) oscillated in amplitude synchronously with the sputter. This sound could also be produced when the machine was shut off and the specimen was flexed by hand-turning the cams. In this case the sound was associated with the part of the cycle during which crack closure was occurring.

5. DISCUSSION

5.1 SEPARATION OF NOISE SOURCES

In this investigation, two simultaneous steps were taken to separate "crack noises" from "machine noises." These steps, described previously, consisted of: (1) inserting acoustic buffers between the specimens and clamps to reduce the amplitude of extraneous noises reaching the acoustic transducers, and (2) separating remaining machine noises by electronically filtering out signals that were outside the frequency range identified as predominantly occupied by crack noises. Insertion of the buffer materials and appropriate choice of signal amplification served to reduce the higher-frequency machine noises to a level that was insignificant compared to noise emanating from the crack.

With these relatively simple precautions, it was found that in the two frequency bands used (100 to 300 and 300 to 1000 kHz) the acoustic emissions were attributable to crack noises. Machine noises were predominantly in the range below 100 kHz. This was confirmed by cycling a number of specimens that contained no notch or other known crack sources. One unnotched aluminum alloy specimen was cycled for several hours, but it was noted that after roughly half an hour the acoustic emission count rate was nil. This effect is also shown in Figs. 5 and 7 for the unnotched titanium alloy and maraging steel specimens. This "settling-out" effect* would not have occurred had machine noises imposed themselves in the frequency bands assigned to the transducer channels. However, when these same specimens were notched and reinserted into the fatigue machine, the acoustic emission counts continued to accumulate with crack growth (figs. 5, 6, and 7). Table I contains additional evidence that the acoustic emission counts did not simply accumulate as a result of continued application of load cycles. Thus, the cumulative kilocounts to fracture appear to be entirely characteristic of the materials tested rather than of the machine noises. However, the kilocounts quoted in table I should be taken only as order-of-magnitude values indicating the

*The source of the small amount of initial noise produced by the unnotched specimens was not determined in these tests.

differences between the materials since only a few specimens were actually tested.

5.2 NATURE OF CRACK NOISES

Although it was not confirmed in these tests, we postulate that the predominant source of acoustic emission was due to fracture surface interaction (i.e., crack closure) rather than to crack extension or plastic deformation.[11,16] It was observed that considerably more emission counts were generated by rougher fracture surfaces. The least counts were accumulated with the maraging steel which exhibited a homogeneous and "smooth" fracture surface (see table I and fig. 8(c)). The aluminum alloy initially accumulated counts at rates as low as the maraging steel (see fig. 6), and then the counts accumulated very rapidly as the fresher fracture surface became progressively rougher (see fig. 8(b)). The titanium alloy exhibited a rough fracture surface throughout the test, and this was attended by a consistently-higher cumulative count (see figs. 5 and 8(a)).

One of the factors that can affect the amplitude and count rate of acoustic emissions is the morphology of the material in which crack growth is occurring.[17] However, these tests seemed to indicate that emission occurred even with no crack growth since additional acoustic emission counts could be generated by hand-turning the cams through the crack closure part of a cycle. Thus, there appears to be some preliminary support for the argument that fracture surface interaction is an important source of acoustic emissions in these tests.

If this argument is valid, then the following model for acoustic emission crack detection gains support. In a noisy environment plastic deformation and micro-cracking may escape detection because of the low amplitude of these emissions; where as, fracture surface interactions may produce more pronounced emissions. In this case, the promotion of fracture surface interactions via cyclic loading might be relied upon to announce the presence or growth of a crack. Validation of this model awaits further experimental evidence from tests in which an existing crack is detected under essentially zero crack growth conditions.

Another question to be resolved is implicit in the results obtained with the minimally-cracked specimens. The plots for the titanium and aluminum alloys in Figs. 9 and 10 show significant increases in count rate at the half-crack length grew to 0.05 cm (0.02 in.). This kind of increase in the acoustic emission count rate is usually explained by asserting that there is an associated abrupt increase in crack growth. However, this explanation is not supported by the ultrasonic evidence. Our ultrasonic crack monitoring showed uniform and continuous crack growth, at least on a macroscale. This apparent lack of direct correlation between acoustic emissions and crack growth has been noted by other investigators, but the reason for it is not known.[11]

A further question concerns the signal transmission properties of the specimens and the nature of the frequency spectra observed. The spectrum shown in Fig. 12 is typical of the frequency bandwidth that can be sustained in a plate specimen subjected to simulated acoustic emission centered at roughly 1 MHz.[18] In any bounded medium such as the plate specimens used in these tests, dispersion effects can substantially alter (i.e., shift) the frequency content of the signals. Therefore, the frequency spectra obtained in these tests may be peculiar to the specimens used. Moreover, spectra can apparently become altered as the source of emission changes, say, from plastic deformation to crack extension.[19] Although some variations in the spectra were observed, none were clearly associated with changes in the acoustic emission count rate. Nor was there serious attenuation of these signals within the bandwidths used over a distance of at least the order of half the specimen length of about 15 cm (~6 in.). Reference 18 indicates that effective transmission of this type of signal should be expected over even greater distances (to the order of at least 60 cm (~24 in.) in aluminum alloys).

5.3 APPLICABILITY OF RESULTS

The prospect of acquiring acoustic emission indications of small cracks in actual rotating parts via fracture surface interactions appears to be worth further study in view of the previously discussed results. The data generated to this point indicate that the titanium and aluminum alloys tested will produce the clearest crack signals as opposed to the maraging steel which is a relatively quiet material even when large cracks are present. But further study will be needed before cyclic loading can be exploited for crack detection and monitoring.

In general, it appears that the application of acoustic emission in cyclic loading situations may afford an opportunity for detecting and studying fatigue cracks. It should be noted, however, that preliminary results of the type given herein cannot be used to assert that a particular number of cumulative counts indicate a crack of a particular size in a particular material.

6. SUMMARY OF RESULTS

These preliminary results indicate that acoustic emission measurements can be used as a tool for detecting the presence of fatigue cracks in plate specimens subjected to cyclic bending in a relatively noisy environment. Materials tested were 6Al-4V titanium, 2219-T87 aluminum, and 18-Ni maraging steel. Both notched and unnotched specimens were utilized. The following results were obtained.

1. The data appear to indicate that fracture

surface interaction (crack closure) noise is a source of acoustic emission that may be useful to indicate the presence of cracks while the specimen is being subjected to cyclic loading.

2. For the same number of loading cycles, the cumulative total of acoustic emission counts obtained from a notched specimen is much greater than from an unnotched (or uncracked) specimen. A relatively small amount of acoustic emission was observed with unnotched specimens early in the test, after which no increase in acoustic emission was observed. Upon introducing a notch, acoustic emission increased significantly and continued to do so until the test was terminated.

3. The texture of the fracture surface appeared to have a significant effect on the amount of acoustic emission measured. For example, a maraging steel specimen which exhibited a relatively smooth fracture surface produced about 50 cumulative kilocounts of acoustic emission when run to fracture, while aluminum and titanium alloys with progressively rougher fracture surfaces produced 1500 and 4500 kilocounts, respectively, while the number of fatigue cycles to fracture range from approximately 200 to 300 kilocycles. It is this crack-surface-roughness property, therefore, that may be instrumental in determining which materials are most likely to emit crack-warning signals when actual parts are being tested.

4. The acoutic emission emanating from the specimens was in the frequency range of 100 to 400 kHz while the machine noises were predominantly in the frequency range below 100 kHz. Thus, in a noisy environment as in a bending fatigue machine, extraneous noises can be expected to be different in frequency content and amplitude and not interfere with acoustic emission signals of interest.

7. REFERENCES

1. Tetelman, A. S.: Acoustic Emission and Fracture Mechanics Testing of Metals and Composites. Rep. UCLA-ENG-7249, Univ. California, Los Angeles, (AROD-8016-6-MC, AD-746261), July 1972.

2. Frederick, J. R.: Use of Acoustic Emission in Nondestructive Testing. Univ. Michigan, College of Eng. (AFML-TR-72-114), Oct. 1972.

3. Moore, J. F.; Tsang, S.; and Martin, G.: The Early Detection of Fatigue Damage. North American Rockwell Corp. (AFML-TR-71-185, AD-730348), Sept. 1971.

4. Nakamura, Y.; McCauley, B. O.; and Veach, C. L.: Study of Acoustic Emission During Mechanical Tests of Large Flight Weight Tank Structure. Rep. MSC-04800, FZK-390, General Dynamics Corp. (NASA CR-115761), Mar. 15, 1972.

5. Jolly, W. D.: Acoustic Emission Exposes Cracks During Welding. Welding J., vol. 48, no. 1, Jan. 1969, pp. 21-27.

6. Balderson, H. L.: The Broad Range Detection of Incipient Failure Using the Acoustic Emission Phenomena, Acoustic Emission, Spec. Tech. Publ. No. 505, ASTM, 1972, pp. 297-317.

7. Nakamura, Y.: Acoustic Emission Monitoring System for Detection of Cracks in a Complex Structure. Materials Evaluation, vol. 29, no. 1, Jan. 1971, pp. 8-12.

8. Smith, S.; and Morton, T. M.: Acoustic Emission Detection Techniques for High Cycle Fatigue Testing. Paper No. 2059A, Society for Experimental Stress Analysis Fall Meeting, Seattle, Wash., Oct. 17-20, 1972.

9. Dunegan, H. L.; Harris, D. O.; and Tetelman, A. S.: Detection of Fatigue Crack Growth by Acoustic Emission Techniques. Materials Evaluation, vol. 28, no. 10, Oct. 1970, pp. 221-227.

10. Liptai, R. G.; Harris, D. O.; Engle, R. B.; and Tatro, C. A.: Acoustic Emission Techniques in Materials Research. Int. J. Nondestructive Testing, vol. 3, 1971, pp. 215-275.

11. Harris, D. O. and Dunegan, H. L.: Continuous Monitoring of Fatigue Crack Growth by Acoustic Emission Techniques. Tech. Rep. DE-73-2, Dunegan-Enderco, Livermore, Calif., Feb. 1973.

12. Engle, D. M.; Mitchell, J. R.; Bergey, K. H.; and Appl, F. J.: Acoustic Emission for Monitoring Fatigue Crack Growth. Proceedings of the 27th Annual Conference of the Instrument Society of America, 1972, pp. 638-1 to 7.

13. Hutton, P. H.: Acoustic Emission Applied to Determination of Structural Integrity. Rep. BNWL-SA-3147, Battelle Memorial Inst., Mar. 1972.

14. Hutton, P. H.; and Ord, R. N.: Acoustic Emission. Research Techniques in Nondestructive Testing. R. S. Sharpe, ed., Academic Press, 1970, pp. 25-30.

15. Klima, S. J.; Lesco, D. J.; and Freche, J. C.: Ultrasonic Technique for Detective and Measurement of Fatigue Cracks. NASA TN D-3007, 1965.

16. Elber, W.; The Significance of Fatigue Crack Closure. Damage Tolerance in Aircraft Structures. Spec. Tech. Publ. No. 486, ASTM, 1971, pp. 230-242.

17. Dunegan, H. L.; and Green, A. T.: Factors Affecting Acoustic Emission Response from Materials. Acoustic Emission. Spec. Tech. Publ. No. 505, ASTM, 1972, pp. 100-113.

18. Fowler, K. A.; and Papadakis, E. P.: Observation and Analysis of Simulated Ultrasonic Acoustic Emission Waves in Plates and Complex Structures. Acoustic Emission. Spec. Tech. Publ. No. 505, ASTM, 1972, pp. 222-237.

19. Graham, L. H.; and Alers, G. A.: Frequency Spectra of Acoustic Emissions Generated by Deforming Metals and Ceramics. North American Rockwell Science Center, Thousand Oaks, Calif., Sept. 1972.

TABLE I. - SUMMARY OF ACOUSTIC EMISSION DATA FOR THREE FATIGUE SPECIMENS TAKEN TO FRACTURE

MATERIAL	MAX CYCLIC STRESS[a]		STRESS RATIO[b]	KILOCYCLES TO FRACTURE[c]	KILOCOUNTS AT FRACTURE[c, d]
	MN/M^2	KSI			
Ti 6Al-4V	450-480	65-70	0.6	315	4500
Al 2219-T87	170-210	25-30	.4	235	1500
MARAGING STEEL	~860	~125	.5	220	50

[a]CALCULATED STRESS ON TOP SURFACE OF SPECIMEN (APPROXIMATELY 45% OF THE MATERIAL YIELD STRENGTH).
[b]RATIO OF MIN TO MAX STRESS DURING CYCLING IN TENSION-TENSION MODE.
[c]TOTAL NO. OF FATIGUE CYCLES & ACOUSTIC EMISSION COUNTS WHEN CRACK TIP REACHED EDGE OF SPECIMEN ON EITHER SIDE OF THE STARTER NOTCH.
[d]ACOUSTIC EMISSION WAS MONITORED AT A 100 TO 300 kHz BANDWIDTH & TOTAL GAIN OF 77 dB FOR EACH MATERIAL.

CS-66481

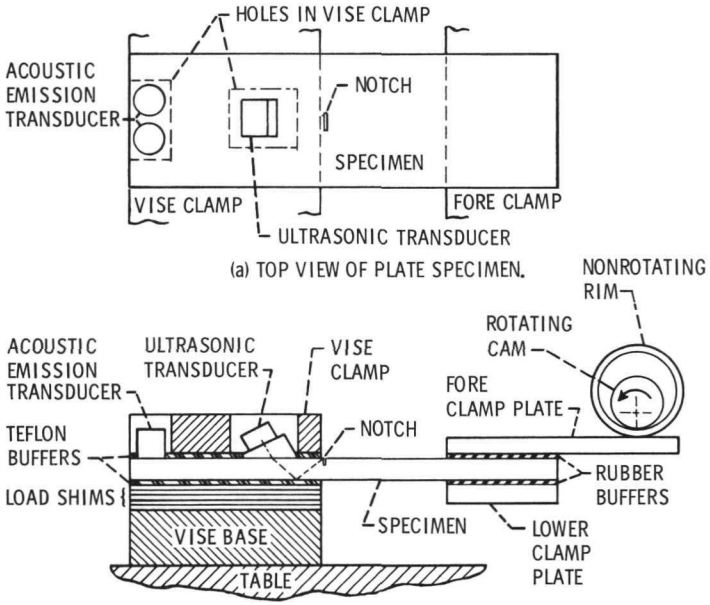

Figure 2. - Diagram of bending fatigue machine and transducer arrangement.

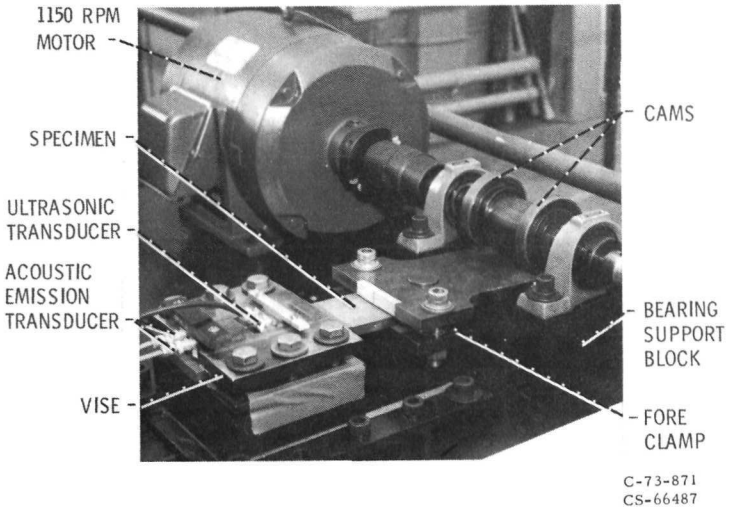

Figure 1. - Bending fatigue machine and related apparatus.

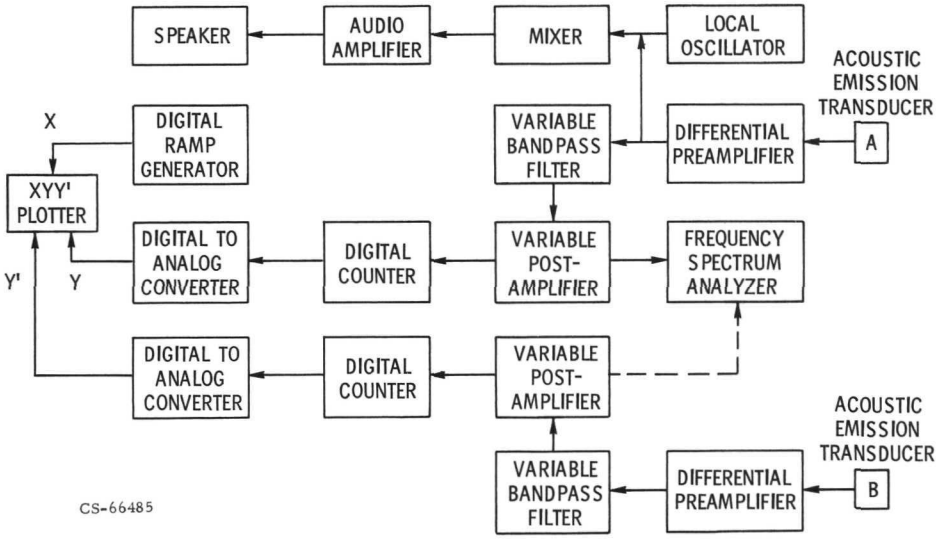

Figure 3. - Schematic of acoustic emission monitor system.

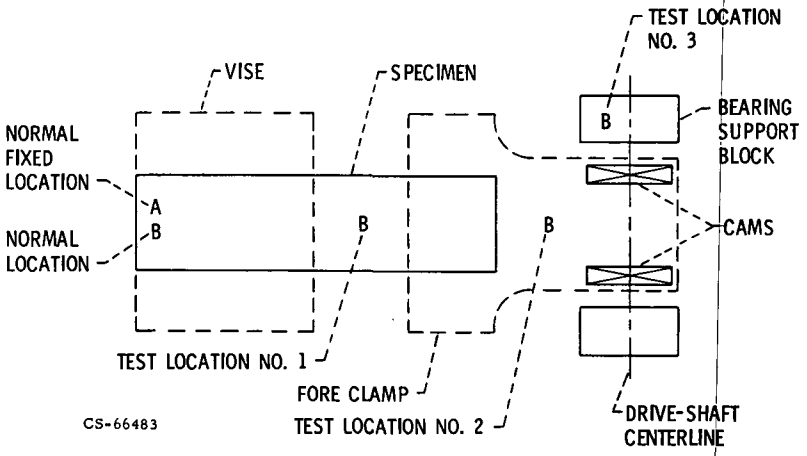

Figure 4. - Test locations of roving acoustic emission transducer (B).

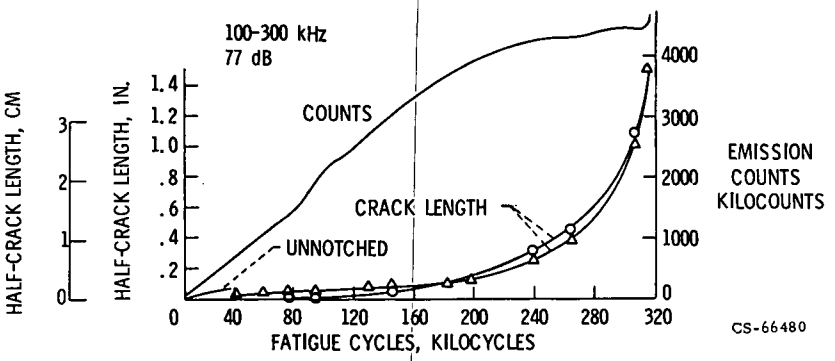

Figure 5. - Acoustic emission counts and crack length as a function of fatigue cycles for 6Al-4V-titanium specimen taken to full fracture.

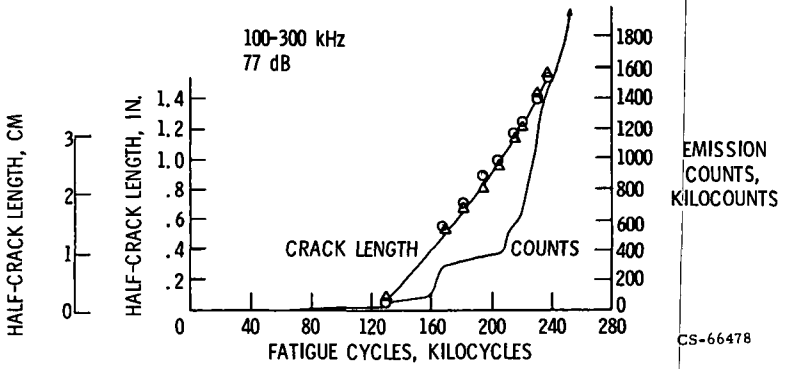

Figure 6. - Acoustic emission counts and crack length as a function of fatigue cycles for 2219-T87 aluminum specimen taken to full fracture.

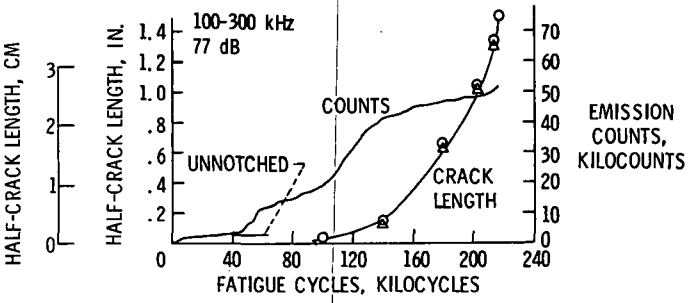

Figure 7. - Acoustic emission counts and crack length as a function of fatigue cycles for 18-Ni maraging steel specimen taken to full fracture.

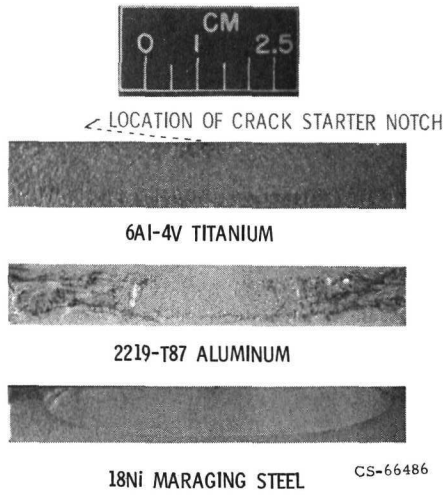

Figure 8. - Specimen fracture surfaces.

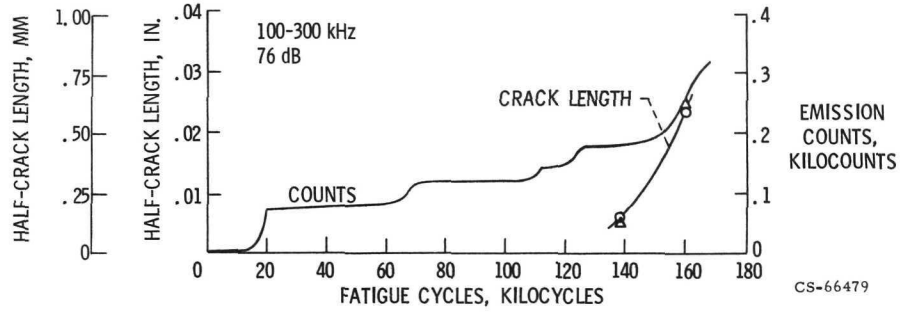

Figure 9. - Acoustic emission counts and crack length as a function of fatigue cycles for minimally cracked 6AI-4V titanium specimen.

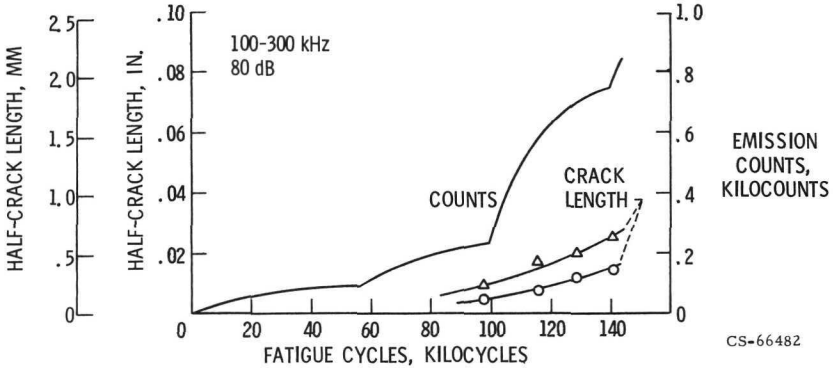

Figure 10. - Acoustic emission counts and crack length as a function of fatigue cycles for minimally cracked 2218-T87 aluminum specimen.

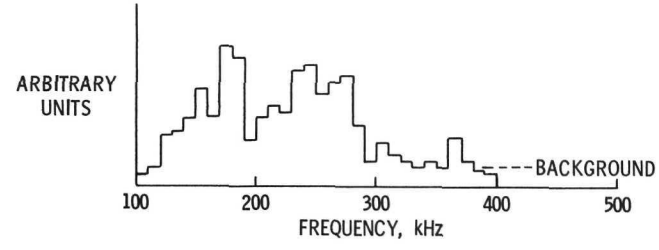

Figure 11. - Typical frequency spectrum for titanium plate specimens in bend fatigue machine.